Superconductivity

Luis A. Flores & María Ramos
University of Puerto Rico at Río Piedras
FISI 4077 Intermediate Laboratory
Dr. Ratnakar Palai

Abstract
The purpose of this experiment was to understand the theoretical aspects of superconductivity by studying the phenomenon through the Meissner-Ochsenfeld effect and SQUID magnetometer. The critical temperatures for three superconductors were found with errors of 2.73%, 3.75%, and 2.44% allowing for an accurate identification of the materials. Furthermore, a reasonable I-V curve was obtained for the SQUID when compared to the theoretical curve.

1 Introduction

Superconductivity was discovered in 1911 by Dutch physicist H. Kamerlingh Onnes who studied the resistance of mercury using liquid helium *(fig.1)*. Superconductivity indicates zero electrical resistance and an expulsion of magnetic fields in materials that are cooled below a characteristic critical temperature *(fig. 2)*. Onnes observed an abrupt disappearance in mercury's electrical resistance at 4.2K and the superfluid transition of helium at 2.2K. At the time, it was understood that most metals could not become superconductors at temperatures higher than 23K making of liquid helium the required refrigerant to observe and study superconductivity. In this experiment, a review of the proposed theories of superconductivity are studied along with some of the experimentations that support them.

2 Theoretical Background

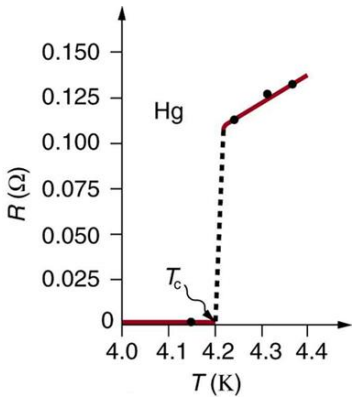

Figure 1. Temperature-Resistance graph of mercury displaying an abrupt change in resistance at 4.2K.

In 1933, German physicists W. Meissner and R. Ochsenfeld observed that superconductors expelled applied magnetic fields during superconducting state transitions *(fig. 3)*. This effect is known as the Meissner-Ochsenfeld effect *(fig. 2)*. Later in 1935, German-British physicists Fritz and Heinz London developed the London theory; a phenomenological theory of superconductivity. The London brothers were able to explain the Meissner-Ochsenfeld effect because of the minimization of the electromagnetic free energy carried by superconducting current.

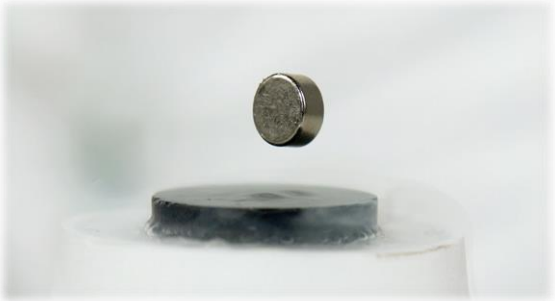

Figure 2. Meissner effect. Magnetic rare earth metal levitating above a superconducting material that has reached critical temperature.

In 1950, Russian-Soviet physicists D. Landau and L. Ginzburg created a macroscopic theory of superconductivity known as the Ginzburg-Landau theory. Furthermore, the dependency of critical temperature on the isotopic mass of a superconductor was discovered the same year. This led to an electron-phonon interaction as a microscopic mechanism for superconductivity. American physicists J. Bardeen, L. Cooper, and J. Schrieffer developed a complete microscopic theory of superconductivity in 1957 known as the BCS theory. This theory explains superconducting current as a superfluid of cooper pairs, pairs of

electrons interacting through the exchange of phonons. The theory also forbade superconductivity at temperatures above 30K. In 1986, German and Swiss physicists J. Bednorz and K. Müller discovered superconductivity in a lanthanum cuprate perovskite material at 35K. Later, it was found that by replacing the lanthanum with yttrium (YBCO) the material was superconducting at 90K allowing the use of liquid nitrogen (77K) as a refrigerant which is easier to attain and maintain. Several contributions and theoretical predictions have been made following BCS theory i.e., the Josephson effect, high temperature superconductivity, and super-insulators. In 2015, hydrogen sulphide was observed to exhibit superconductivity at near 203K but at pressures of 150 gigapascals.

3 The Meissner Effect

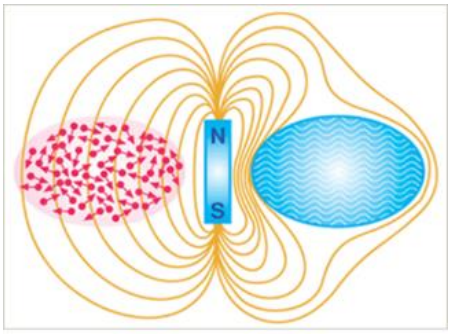

Figure 3. Comparison between a conductor (left) and a superconductor (right) when exposed to an external magnetic field.

In a weak applied field, a superconductor expels nearly all magnetic flux by setting up electric currents near its surface *(fig. 3)*. The magnetic field of these surface currents cancels the applied magnetic field within the bulk of the superconductor. An external field can penetrate the superconductor but only to a very small distance known as the London penetration depth. Each superconductor material has its own characteristic depth. In an ordinary electrical conductor, incoherent and disordered electrons allow the infiltration of an external magnetic field. In a superconductor, coherent collective functioning of the electrons spontaneously excludes external magnetic fields maintaining an impenetrable status. From London theory, one can obtain the dependence of the magnetic field inside the superconductor on the distance to the surface. The London penetration depth decays exponentially to zero within the bulk of the material and for most superconductors, this depth is on the order of 100nm. From London theory we have several equations that explain the behaviour of superconductors. For these equations, the parameter j_s corresponds to the superconducting current density, B to the magnetic field within a superconductor, e is the charge of an electron, m the electron mass, n_s is a phenomenological constant associated with number density of superconducting carriers, μ_0 permeability of free space, λ the London penetration depth, and H the magnetic field.

$$\nabla^2 H = \lambda^{-2} H \tag{1}$$

$$\nabla \times j_s = -\frac{n_s e^2}{m} B \tag{2}$$

$$\nabla \times B = \mu_0 \mathrm{j} \tag{3}$$

$$\lambda = \sqrt{\frac{m}{\mu_0 n_s e^2}} \tag{4}$$

$$\nabla^2 B = \frac{B}{\lambda^2} \tag{5}$$

The electromagnetic free energy in a superconductor is minimized following London equation *(eq. 1)* which predicts that the magnetic field in the superconductor decays exponentially from the value it has at the surface. The London equation *(eq.2)* can be manipulated by using Maxwell's equations *(eq. 3)* to obtain the penetration depth *(eq. 4)*, which defines a characteristic length over which external magnetic fields are exponentially suppressed. By Maxwell's equations, the value for the magnetic field inside the superconductor must be identically zero *(eq. 5)* unless the penetration depth is infinite, which is not the case for superconductors.

4 Ginzburg-Landau Theory

In superconductors, a transition from the superconducting state to a normal state will have a transition layer of finite thickness

which is related to a coherence length. The superconducting coherence length, usually denoted ξ, is the characteristic exponent of the variations of the density of superconducting component. It is given by

$$\xi = \sqrt{\frac{\hbar^2}{2m|a|}}, \tag{6}$$

where α is a constant. This quantity is related to the Fermi velocity for the material and the energy gap associated with the condensation to the superconducting state. The superconducting electron density cannot change quickly and there is a minimum length over which a given change can be made, lest it destroys the superconducting state. The ratio

$$k = \frac{\lambda}{\xi}, \tag{7}$$

where λ is the London penetration depth, is known as the Ginzburg-Landau parameter.

5 Bardeen-Cooper-Schrieffer Theory

This theory describes superconductivity as a microscopic effect caused by a condensation of Cooper pairs into a boson-like state. It explains the phenomenon in which a current of electron pairs flows without resistance in certain materials at low temperatures *(fig. 4)*. Furthermore, it is used in nuclear physics to describe the interaction between nucleons in atomic nuclei. A key conceptual element in this theory is the pairing of electrons close to the Fermi level into Cooper pairs through interaction with the crystal lattice. This pairing results from a slight attraction between the electrons related to lattice vibrations; the coupling to the lattice is called a phonon interaction. This coupling is viewed as an exchange of phonons, phonons being the quanta of lattice vibration energy.

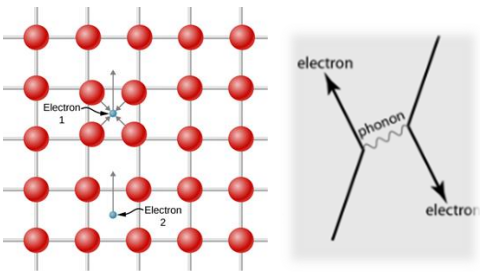

Figure 4. A visual model of a Cooper pair attraction and its Feynman diagram.

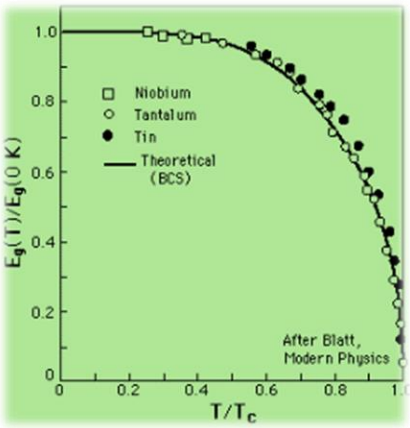

Figure 5. Energy gap in superconductors as a function of temperature.

The evidence for a small band gap at the Fermi level was a key piece in BCS theory. This evidence comes from the existence of a critical temperature, the existence of a critical magnetic field, and the exponential nature of the heat capacity variation in Type I superconductors. The band gap suggested a phase transition in which there was a kind of condensation, but electrons alone cannot condense into the same energy level because of Pauli exclusion principle. The BCS theory predicts a bandgap of

$$E_g = \frac{7}{2} kT_c, \tag{8}$$

where T_c is the critical temperature for the superconductor and the energy gap is related to the coherence length for the superconductor. The reduction of the energy gap as a SC approaches critical temperature can be taken as an indication that the charge carriers have some form of collective nature *(fig.5)*. This kind of evidence, along with the isotope effect which showed that the crystal lattice was involved, helped to suggest the picture of paired electrons bound together by phonon interactions with the lattice.

6 Experimental Theory & Equipment

Part I: Meissner Effect

This experiment consisted of two parts which were completed as a group effort given the limited amount of liquid nitrogen to study the effects of superconductivity. The first part consisted of studying the Meissner effect by measuring the critical temperature of three

ceramic superconductors. The apparatus used in this experiment was composed of three thermocouple leads *(fig.6)* connected to three superconductors, four rare earth metals *(fig.8)*, a multimeter, liquid nitrogen and a foam cube. Plastic tweezers were used to manipulate the samples and banana cables were used to plug the multimeter. For these superconductors the critical temperature is about 90K for $YBa_2Cu_3O_7$, 80K for $Bi_2Sr_2Ca_{n-1}Cu_nO_9$ with n=2, and 110K with n=3. It is not clear however that these ceramic superconductors conduct electricity by means of Cooper Pairs as described by BCS theory. The Resonant Valence Bond theory has been more effective in explaining the gradual onset of superconductivity at critical temperatures in ceramic materials. The temperature can be accurately measured with thermometers designed and calibrated for use in the temperature range of interest. Highly accurate thermometers typically do not operate over such a wide range. Thermocouple thermometers however are accurate over this large temperature variance.

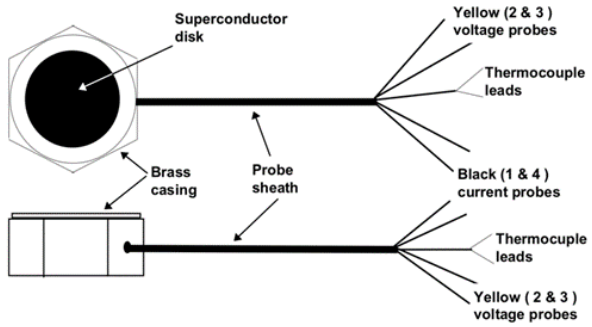

Figure 6. Diagram of thermocouple leads.

A thermocouple consists of a mechanical junction of two dissimilar metals *(fig. 6)*. This junction generates a small electrical potential (voltage), the value of which depends upon the temperature of the junction. Thus, with calibration, and an appropriate choice of metals, one can obtain a thermometer for the desired temperature range. For our range of 300K to 77K a type T or Copper-Constantan thermocouple is used. A -0.16mV reading indicates room temperature (298K), and +6.43mV corresponds to 77K. The thermocouple junction has been carefully attached to the superconductors in our kits, and thermally balanced and calibrated to be used with the table below at 70°F.

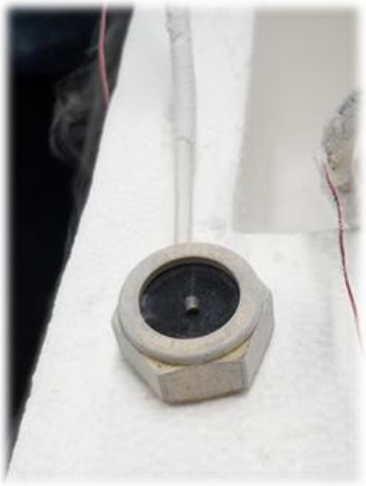

Figure 7. Example of a rare earth metal in one of the superconductors connected to a thermocouple lead.

A digital millivoltmeter attached to the leads can be used to determine the voltage of this junction. Note that thermocouple leads must be connected to the voltmeter via wires of the same material and the junction to the thermocouple leads must be at room temperature *(fig.7)*. This voltage can be converted to the equivalent temperature with the help of the conversion chart provided in the instruction manual.

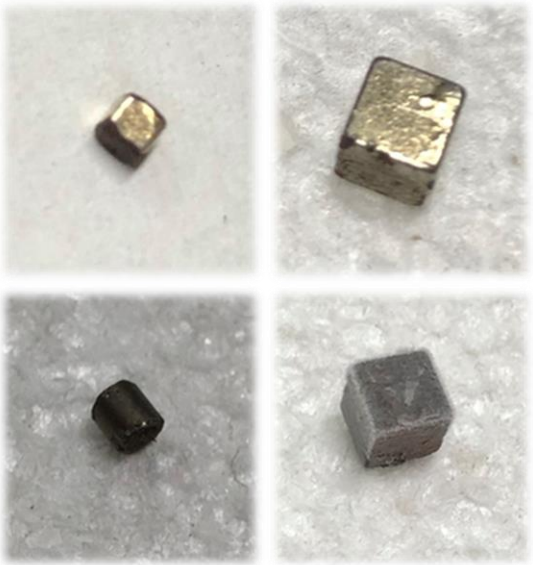

Figure 8. Samples described as small cube, big cube, cylinder, and black cube for identification purposes.

Part II: DC SQUID

For the second part of the experiment to study superconductivity we used DC SQUID; a

direct current superconducting quantum interference device magnetometer having a high temperature superconductor thin-film chip, two feedback coils to modulate the SQUID and to couple an external signal to the SQUID, a cryogenic probe with a removable magnetic shield, an electronic control box containing all the circuits needed to operate the SQUID, and a cable to connect the probe to the electronics box *(fig.9)*. The probe is designed to be immersed in a liquid nitrogen bath in the included flask. Inside is a small integrated circuit chip whose main components are a DC SQUID and two feedback coils. The SQUID is made of yttrium barium copper oxide (YBCO) that is fashioned into a ring containing two active devices called Josephson junctions. The devices and structures on the chip are created using the same photolithographic steps that are used in the integrated circuits (IC's) that dominate today's conventional electronic devices. The apparatus can be used to detect small magnetic signals if they are properly coupled to the SQUID, but it does not have the sensitivity of high-performance laboratory SQUIDs.

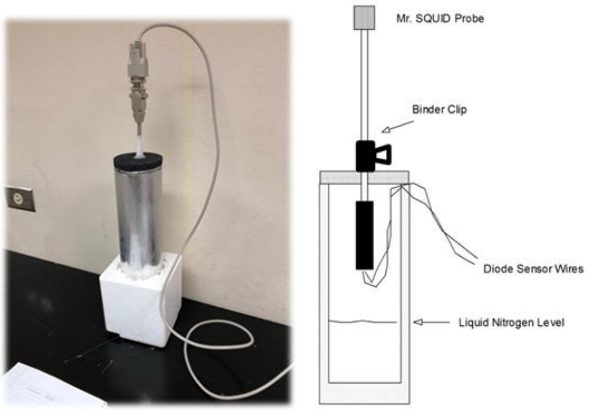

Figure 9. DC SQUID aparattus and diagram.

English physicist Brian D. Josephson predicted the flow of current in 1962 based on the BCS theory of superconductivity. The subsequent experimental verification of the Josephson effect lent support to the BCS theory. Josephson junctions occur when two superconductors are weakly coupled together which causes them to behave like superconductors that can only carry a small amount of zero-voltage current before it becomes resistive. All superconductors exhibit their special properties until a critical temperature is reached, that limit also exist with the amount of current. The maximum value a superconductor can carry is called the critical current. This Josephson effect is a manifestation of the long-range quantum coherence of superconductors. In this case, two regions of superconductor are placed very close to one another separated only by a thin gap. Any weak coupling between two regions of superconductor therefore exhibits the Josephson effect. Each superconductor region has a different quantum mechanical phase, normally unrelated, but in this case, they have a specific relationship which assures a lower energy ground state that results in superconductivity. The regions act like a single superconductor where electrical currents can flow between the two regions with zero resistance. This current is called Josephson current and this property is what causes physical systems composed of two regions of superconductor to be called Josephson junctions. Josephson currents are a manifestation of the DC Josephson effect.

The Josephson effect is central to the operation of the SQUID which is a very sensitive detector of magnetic fields. DC SQUIDs consist of two Josephson junctions connected in parallel on a closed superconducting loop. An important property of superconducting rings is that they can enclose magnetic flux only in multiples of a universal constant called the flux quantum, and, because the flux quantum is very small, this physical effect can be exploited to produce this extraordinarily sensitive magnetic detector.

7 Data & Results

Part I: Meissner Effect

The four samples *(fig.8)* were placed in the different superconductor disks which were labelled A, B, and C *(fig.7)*. We measured voltage in mV and the equivalent temperature was found with the equivalence table provided by the manual. The following tables *(table1, 2, 3, 4)* gather the data corresponding to each of the samples when placed in the different disks. In *(table2)* we can see that the cylindrical sample had little or no levitation in disks A and B. However, in disk C the cylinder levitated at 79K and dropped at 107K. Similar results can

be seen for the other samples showcasing the Meissner effect.

Small Cube					
A (mV)	°K	B (mV)	°K	C (mV)	°K
6.34	79	6.37	78	6.33	79
6.3	79	6.34	79	6.31	80
6.09	85	6.31	80	6.18	83
5.93	89	6.28	80	5.84	92
5.77	94	6.25	81	5.63	97
5.6	98	6.23	82	5.46	101
5.45	102	6.21	82	5.3	106
		6.17	83	5.2	109
		6.12	84		

Table 1. Voltage-Temperature data for the small cube sample when placed in the different superconducting disks.

Cylinder					
A (mV)	°K	B (mV)	°K	C (mV)	°K
6.35	78.5	6.37	78	6.32	79
				6.27	80.5
				6.25	81
				5.92	89
				5.69	96
				5.52	100
				5.36	104
				5.28	107

Table 2. Voltage-Temperature data for the cylinder sample when placed in the different superconducting disks.

Black Cube					
A (mV)	°K	B (mV)	°K	C (mV)	°K
6.38	78	6.32	79	6.38	78
		6.31	79.5	6.27	80.5
		6.28	80	5.95	88.5
		6.26	80.5	5.74	94
		6.24	81	5.55	99
		6.22	81.5	5.38	104
		6.2	82		

Table 3. Voltage-Temperature data for the black cube sample when placed in the different superconducting disks.

Big Cube					
A (mV)	°K	B (mV)	°K	C (mV)	°K
6.27	79.5	6.34	79	6.43	77
6.19	82.5	6.34	79	6.39	77.5
		6.31	79.5	6.38	78
				6.08	85
				5.8	91.5
				5.61	98
				5.46	101.5

Table 4. Voltage-Temperature data for the big cube sample when placed in the different superconducting disks.

The data *(table1)* corresponding to the small cube indicates that the sample levitated in all superconducting disks around 78K. Therefore, all superconductors were in the Meissner state at this temperature. To find the critical temperature of the superconductors, the samples were observed until the levitation effect ended. These temperatures correspond to the last entry of the data for each superconducting disk. For the small cube, the Meissner effect stopped at 102K, 84K, and 109K for disks A, B, and C respectively. The four-probe technique could have been used to measure the resistance of the superconductors, but this part was not done. However, the instruction manual provided the critical temperatures of the materials *(Section6)*. From this data, it appears that disk A can be identified as $YBa_2Cu_3O_7$, while disk B corresponds to $Bi_2Sr_2Ca_1Cu_2O_9$, and disk C to $Bi_2Sr_2Ca_2Cu_3O_9$ by comparison of experimental temperatures with the ones provided in the manual. It can be observed that for other rare earth samples, superconductor disk C stays with a high critical temperature and disk B has the lowest. Therefore, the previous identification of the superconductors must be correct if we follow this data.

Part II: SQUID

A current-voltage graph was created using the data taken from the oscilloscope to obtain the SQUID curve. In *(fig.10)*, we can observe how the graph increases rapidly, then it becomes somewhat constant and then increases again behaving somewhat like a cubic function. When using the SQUID without liquid nitrogen, its I-V characteristic curve would be a straight line because the junctions behave like ordinary resistors. The non-linear shape shown in *(fig.10)* indicates the presence of a non-resistance current flowing through the Josephson junctions once the junctions are cooled and behaving like superconductors. This exhibits the DC Josephson effect where a non-resistance current flows through a Josephson junction. However, a flat region on the curve should correspond to current flowing with no voltage which is called a supercurrent, but this region is not easily visible.

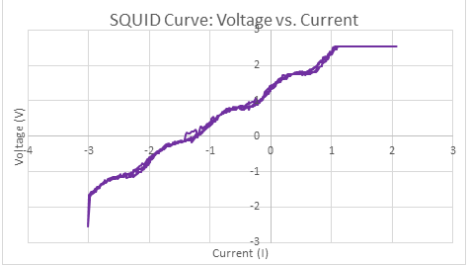

Figure 10. Current-Voltage graph for the SQUID curve.

8 Conclusions

Three superconductors were accurately identified by measuring their critical temperatures and observing the Meissner effect with four rare earth metals. The average critical temperatures were calculated to be 107K, 83K, and 92.2K for superconducting disks C, B, and A respectively. These critical temperatures allowed for the identification of disk C as $Bi_2Sr_2Ca_2Cu_3O_9$with a 2.73% of error, disk B as $Bi_2Sr_2Ca_1Cu_2O_9$with 3.75% of error, and disk A as $YBa_2Cu_3O_7$with 2.44% of error. Furthermore, SQUIDs I-V curve was obtained and has a similar aspect to the theoretical I-V curve. Therefore, these experiments support the studied theories of superconductivity.

9 References

[1] "Bardeen-Cooper-Schrieffer (BCS) Theory of Superconductivity." [On- line]. Available: https://jqi.umd.edu/glossary/bardeen-cooper-schrieffer- bcs-theory-superconductivity

[2] "BCS Theory and Superconductivity." [Online]. Available: http://www.phys.ufl.edu/courses/phy4523/spring12/Sample%202.pdf

[3] "Experiment Guide for Superconductor Demonstrations," Colorado Super- conductor Inc.

[4] "The Meissner Effect." [Online]. Available: http://hyperphysics.phy-astr.gsu.edu/hbase/Solids/meis.html

[5] "Mr. SQUID® User's Guide," STAR Cryoelectronics, LLC.

[6] "Superconductivity - The Meissner effect." [Online]. Available: https://www.open.edu/openlearn/science-maths-technology/engineering- and-technology/engineering/superconductivity/content-section-2.3

[7] "BCS theory," Mar 2019. [Online]. Available: https://en.wikipedia.org/wiki/BCS theory

[8] Libretexts, "Meissner effect," Apr 2019. [Online]. Available: https://eng.libretexts.org/Bookshelves/Materials Science/Supplemental Modules (Materials Science)/Magnetic Properties/Meissner Effect